Chapter 2
Piezoelectric Materials

Abstract After some historical remarks the field equations for piezoelectric materials are presented for the 3D and the 2D case. Furthermore, the boundary value problems in bounded and unbounded cracked domains are formulated.

2.1 Short Historical Overview

In the middle of eighteenth century Carolus Linnaeus and Franz Aepinus first observed that certain materials, such as crystals and some ceramics, generate electric charges in case of a temperature change. Both René Just Haüy and Antoine César Becquerel subsequently attempted to investigate the phenomena further but were unsuccessful. Piezoelectricity as a research field in crystal physics was initiated by the brothers Jacques Curie (1856–1941) and Pierre Curie (1859–1906) with their studies, [4, 5]. They discovered an unusual characteristic of certain crystalline minerals as tourmaline, quartz, topaz, cane sugar and Rochelle salt. It was found that tension and compression generated voltages of opposite polarity and proportional to the applied load. This was called by Hankel [13] the piezoelectric effect. The at first discovered direct piezoelectric effect is shown schematically in Fig. 2.1a, b. The word piezoelectricity comes from Greek and means electricity resulting from pressure (Piezo means pressure in Greek). In the year following the discovery of the direct effect, Lippman [22] predicted the existence of the converse effect basing on fundamental thermodynamic principles. Before the end of 1881 the brothers Curies confirmed experimentally the existence of the converse effect. They showed that if one of the voltage-generating crystals was exposed to an electric field it lengthened or shortened according to the polarity of the field, and in proportion to its strength, see Fig. 2.2.

The study of piezoelectricity remained something of a laboratory curiosity for the years until the World War I. In this period it is worth to mention the textbook on

P. Dineva et al., *Dynamic Fracture of Piezoelectric Materials*,
Solid Mechanics and Its Applications 212, DOI: 10.1007/978-3-319-03961-9_2,

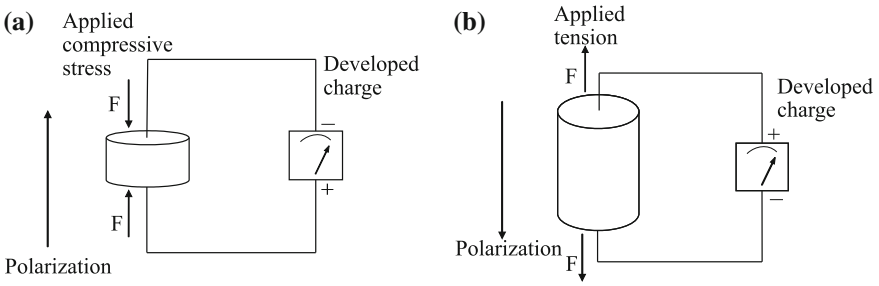

Fig. 2.1 Direct piezo-effect: **a** at applied compressive stress, **b** at applied tension

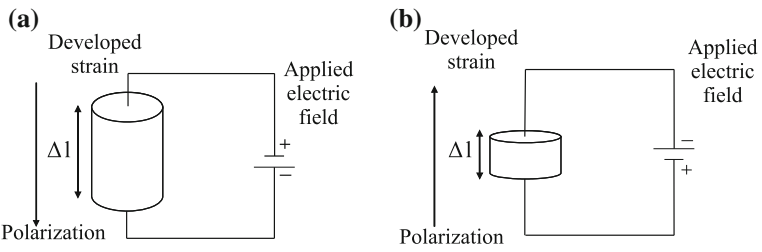

Fig. 2.2 Inverse piezo-effect at applied electric field

crystal physics of Voigt [39] where are described 20 natural crystal classes capable of piezoelectricity with their piezoelectric constants using tensor analysis.

Piezoelectric materials did not come into widespread use until the World War I, when quartz was used as resonators for ultrasound sources in SONAR to detect submarines through echolocation.

A very important stage in the research of piezoelectric materials and especially in their applications in modern engineering practice was the discovery of the phenomenon ferroelectricity by Valasek [38]. Ferroelectric materials exhibit one or more phases and have domain structure in which the individual polarization can be changed by an applied electric field. The first known ferroelectric material was Rochelle salt. Unfortunately, Rochelle salt loses its ferroelectric properties if the composition is slightly changed, which made it rather unattractive for industrial applications. Ferroelectricity was mainly regarded as an interesting physical effect.

During World War II, in the United States, Japan and the Soviet Union, isolated research groups working on improved capacitor materials discovered that certain ceramic materials (prepared by sintering metallic oxide powders) exhibited dielectric constants up to 100 times higher than common cut crystals. Furthermore, the same classes of materials (called ferroelectric) were made to exhibit similar improvements in piezoelectric properties. This led to the manufacturing of synthetic materials whose piezoelectric and dielectric properties are about 100 times higher than the ones of the natural piezoelectric. The discovery of easily manufactured piezoelectric ceramics

with astonishing performance characteristics naturally touched off a revival of intense research and development of piezoelectric devices.

In 1945, piezoelectricity started on the market when it was realized that the mixed oxide compound barium titanate $BaTiO_3$ was a ferroelectric which can easily fabricated and shaped at low price and can made piezoelectric with constants many times higher than natural materials by an electrical poling process. This material is of stable perovskite type, which is one of the fundamental crystal lattice structures. This discovery brought the perovskite type materials into the focus of investigations. Soon other perovskites with ferroelectric properties were discovered, thus opening the path to industrial application. This time could be called the beginning of the era of the piezoelectric ceramic and modern history of piezoelectricity. The following successful results were obtained in the time period 1940–1965:

- Development of the barium titanate family of piezoceramic and the lead zirconate titanate family, see Jaffe et al. [17];
- Development of an understanding of the correspondence of the perovskite crystal structure with electro-mechanical activity;
- Development of a rationale for doping both of these families with metallic impurities in order to achieve desired properties such as dielectric constants, stiffness, piezoelectric coupling coefficients, ease of poling, etc.

Piezoelectricity as one of the branches of crystal physics is now the base of the modern engineering practice in the following technologies:

- Frequency control and signal processing e.g. mechanical frequency filters, surface acoustic wave devices, bulk acoustic wave devices, etc.;
- Sound and ultrasound microphones and speakers, ultrasonic imaging, hydrophones, etc.;
- Actuators and motors based on the converse effect, i.e. when an electric field is applied to a material it will deform in a predictable way. For example, in manufacturing of piezoelectric ceramics it is possible to create rods that deform along the long axis and act like a piston. The amount of deformation can be controlled by the amount of electric field applied to the material. Since the deformations are small, usually within micrometers precision, they are excellent in application that require very small amounts of movement. They have been used as tools for micro precision placement and for micro adjustments in lens for microscopes. The converse effect is used in printers (needle drivers and ink jet), miniaturized motors, bimorph actuators (pneumatics, micropumps, Braille for the blind), multilayered actuators for fine positioning and optics, injection systems in automotive fuel valves, etc.
- Detection of pressure variations in the form of sound is the most common sensor application, e.g. piezoelectric microphones (sound waves bend the piezoelectric material, creating a changing voltage) and piezoelectric pickups for electric guitars. A piezo sensor attached to the body of an instrument or structure is known as a contact microphone giving information of deformation. This is the base of all sensors for strain, mass, flow, pressure online control. By continuously monitoring deformation, the sensors can record operational loads, compute material fatigue, and estimate remaining component life.

- Generator with application in gas and fuel ignition. Piezoelectricity can generate very high voltages but the current is very small. The amount of pressure needed to distort a piezoelectric ceramic element by 0.05 mm can generate nearly 100,000 volts. This amount of voltage is enough to create an electric spark to ignite gas in an oven, grill or pocket lighter.
- Smart structures that use discrete piezoelectric patches to control the response of a structure have been of considerable interest in recent years. The development of modern software makes it possible to fully model coupled thermo–mechanical–electrical systems and obtain reciprocal relations between piezoelectric actuator voltages and system response. By integrating such models into a closed-loop control system, very effective active control on the vibration, noise, shape, deformation, pressure, etc. can be achieved. Structural panels embedded with a series of sensors and actuators can be used in civil, industrial and aerospace structures. These panels can actively monitor the structural integrity and detect faults at early stages, thereby providing precise information on structural failure and life expectancy.
- The concept *Crowd Farm* with the basic idea that large amounts of people moving in dense areas would step on tiles embedded in the floor and these tiles would use piezoelectric materials to generate electricity that could be collected and used. A prototype of the crowd farm has already been tested in a selected number of Japanese train stations.
- Experimental science for investigation of atomistic structure of materials based on the micro-coupling of mechanical and electrical fields.

2.2 Types of Piezoelectric Materials

Piezoelectric materials can be natural or man-made. The natural PEM are crystal materials like quartz ($Si\,O_2$), Rochelle salt, Topaz, Tourmaline-group minerals and some organic substances as silk, wood, enamel, dentin, bone, hair, rubber. Figure 2.3 shows the unit cell of quartz which has specific atomic structure of the lattice which is a tetrahedron built of oxygen atoms around a silicon atom. Each oxygen atom has the same distance to the silicon atom, and the distances between the oxygen atoms are all the same. The change in the position of the atoms due to applied stress leads to the formation of net dipole moments that causes polarization and an electric field, respectively.

Man-made piezoelectric materials are crystals that are quartz analogs, ceramics, polymers and composites.

There are 32 crystal classes which are divided into the following seven groups: triclinic, monoclinic, orthorhombic, tetragonal, trigonal, hexagonal and cubic. These groups are also associated with the elastic nature of the material where triclinic represents an anisotropic material, orthorhombic represents an orthotropic material and cubic are in most cases isotropic materials. Only 20 of the 32 classes alow piezoelectric properties. Ten of these classes are polar, i.e. show a spontaneous polarization without mechanical stress due to a non-vanishing electric dipole moment associated

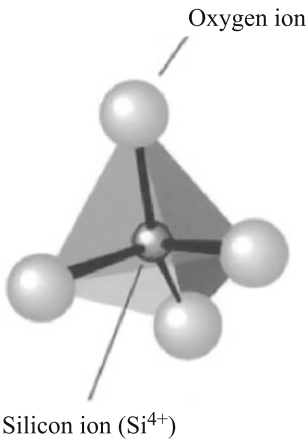

Fig. 2.3 Unit cell of quartz

with their unit cell. The remaining 10 classes are not polar, i.e. polarization appears only after applying a mechanical load.

There are the following families of man-made ceramics with crystal structure as perovskite: Barium titanate ($BaTiO_3$; Lead titanate ($PbTiO_3$); Lead zirconate titanate ($Pb[Zr_xTi_{1-x}]O_3$, $0 < x < 1$)—more commonly known as PZT; Potassium niobate ($KNbO_3$) ; Lithium niobate ($LiNbO_3$); Lithium tantalate ($LiTaO_3$), etc. and other lead-free piezoceramics. The general chemical formulae of perovskite crystal structure is ABO_3 , where A is a larger metal ions, usually lead Pb or barium Ba, B is a smaller metal ion, usually titanium Ti or zirconium Zr, see Fig. 2.4, which shows the crystal structure of a piezoelectric ceramic ($BaTiO_3$) at temperature above and below Curie point.

To prepare a piezoelectric ceramic, fine powders of the component metal oxides are mixed in specific proportions, then heated to form a uniform powder. The powder is mixed with an organic binder and formed into structural elements having the desired shape (discs, rods, plates, etc.). The elements are subsequently fired according to a specific time and temperature program, during which the powder particles sinter and the material attains a dense crystalline structure. The elements are cooled, then shaped or trimmed to specifications, and electrodes are applied to the appropriate surfaces. Above a critical temperature, the *Curie point*, each perovskite crystal in the fired ceramic element exhibits a simple cubic symmetry with no dipole moment, it is in the so-called paraelastic phase (Fig. 2.4a). At temperatures below the Curie point, however, each crystal exhibits a tetragonal or rhombohedral symmetry leading to a dipole moment; this phase of the material is called ferroelectric phase (Fig. 2.4b). When electric field of about 10^6 V/m is applied to the ferroelectric polycrystal as it passes through its Curie temperature, so that its spontaneous polarizations develop, all polarization vectors are aligned in a more or less uniform direction. This process leading to a macroscopic net polarization is called *poling*. Initially there exists a uniform distribution of all direction, i.e. no macroscopic net polarization. After poling: a distribution around the poling direction leads to a macroscopic net polarization.

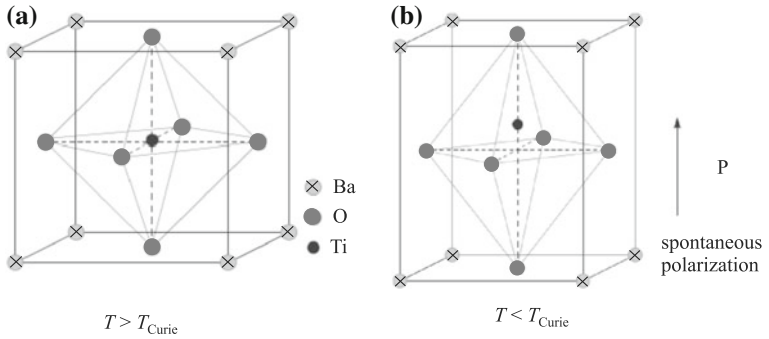

Fig. 2.4 Crystal structure of a traditional piezoelectric ceramic ($BaTiO_3$) at temperature above (**a**) and below (**b**) Curie point

Now, at this stage, when a mechanical stress is applied, the polarization will increase or decrease and the ceramic will have typical piezoelectric behavior. The mechanism of this process will be explained in Sect. 2.3.

The piezoelectricity of polyvinylidene fluoride was discovered by Kawai [18]. PVDF is a ferroelectric polymer, exhibiting piezoelectric and pyroelectric properties. These characteristics make it useful in sensor and battery applications. Thin films of PVDF are used in some newer thermal camera sensors. Piezocomposite materials are an important update of existing piezoceramic, see Newnham [26]. They can be of two types: piezo-polymer in which the piezoelectric material is immersed in an electrically passive matrix (for instance PZT in epoxy matrix) and piezo-composites that are composite materials made by two different ceramics (for example $BaTiO_3$ fibers reinforcing a PZT matrix).

2.3 Physical Peculiarities

Piezoelectric materials are anisotropic dielectrics of special type, where both fields the electrical and the elastic are coupled. Some of them (for instance ceramic) have ferroelectric properties, but the rest of them (as quartz) display no ferroelectric behaviour. In the following a brief explanation is given of the physical properties of dielectrics, ferroelectric, piezoelectric materials and the similarity and difference between them.

A dielectric material is any material that supports charge without conducting it to a significant degree. The main property is that they have no free electrical charges, but when an external electrical field is applied the electric dipoles are being created due to the interaction of the electrical field with the dielectric structure. The electric dipole, see Fig. 2.5 is an electro–neutral unit volume in which the centers of the positive $+q$ and negative $-q$ electric charges (poles) do not coincide and are at distance r, so that the dipole moment $\mu = qr$ arises. The dipole moment is a vector with direction from

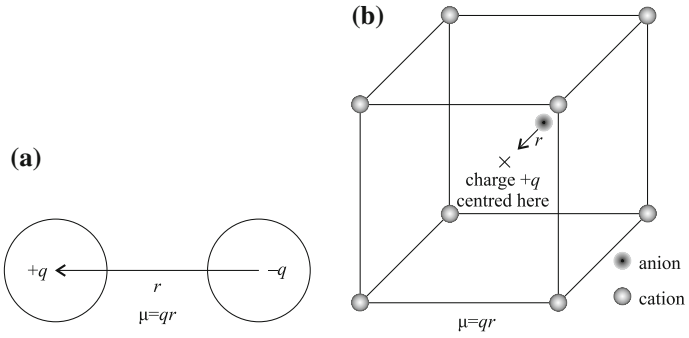

Fig. 2.5 The dipole moment

the negative to the positive pole. Because of dielectric polarization, positive charges are displaced toward the external field and negative charges shift in the opposite direction.

If the center of positive charge within a given region and the center of negative charge within the same region are not in the same position, a dipole moment μ arises. For example, in the Fig. 2.5, the center of positive charge from the eight cations shown is at X, while the center of negative charge is located some distance away on the anion. The second view of dipole moment is more useful, since it can be applied over a large area containing many charges in order to find the net dipole moment of the material.

The polarization of a material is simply the total dipole moment for a unit volume $P = \frac{1}{V}\sum_i \mu_i$, where V is the overall volume of the sample. Because $\sum_i \mu_i$ is a vector sum, a material may contain dipoles without having any net polarization, because dipole moments can cancel out. If a material contains polar molecules, they will generally be in randomly orientated when no electric field is applied, see Fig. 2.6. An applied electric field $E[N/C]$ will polarize the material by orienting the dipole moments of polar molecules in opposite direction—mainly to the applied electrical field E_a. Or, when a dielectric is placed between charged electrode plates, the polarization of the medium produces an electric field E_p opposite to the field of the charges on the plate and then the effective electrical field is: $E_e = E_a - E_p$. The dielectric constant $\varepsilon[C/NM^2]$, which is also called *permittivity*, is the main characteristic of the dielectric. It reflects the amount of reduction of effective electric field as shown in Fig. 2.6. The dielectric constant depends on the polarization properties of the dielectric material, but also on its elastic, thermal, etc. properties. The relative dielectric constant $\varepsilon_\gamma = \frac{\varepsilon}{\varepsilon_0}$ shows how many times the effective electric field decreases in a given dielectric material in comparison with the electric field between the plates when they are in vacuum with a dielectric constant $\varepsilon_0 = 8.85 \times 10^{-12}\,\mathrm{C/Nm^2}$.

Permittivity is directly related to the dimensionless characteristic *electric susceptibility* χ, which is a measure of how easily a dielectric polarizes in response

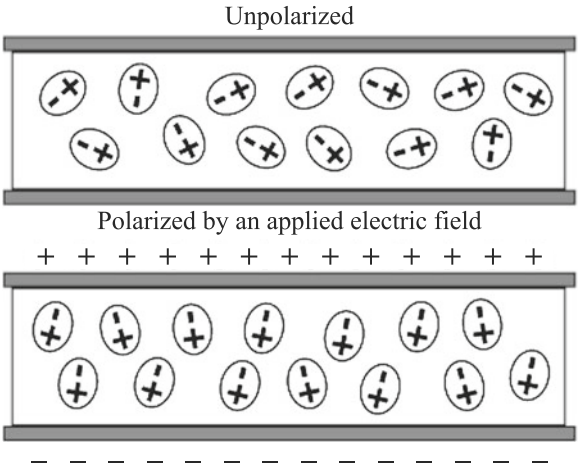

Fig. 2.6 Reduction of an effective electric field due to the polarization

to an electric field. They are related to each other through the scalar relation $\varepsilon = \varepsilon_\gamma \varepsilon_0 = (1+\chi)\varepsilon_0$ for the isotropic case and the tensor relation $\varepsilon_{ij} = (\delta_{ij}+\chi_{ij})\varepsilon_0$ for an anisotropic dielectric materials. An important property of dielectrics is that they posses naturally polarization and in the absence of applied electrical field they have no electric dipoles.

The polarization of piezoelectric material has its specific peculiarities in comparison with polarization of ordinary dielectrics. First we will consider polarization of piezoelectric materials that are not ferroelectric and will discuss the polarization process of quartz as classical representative of this class of materials.

When a piezoelectric is placed under a mechanical stress, the geometry of the atomic structure of the crystal changes, such that ions in the structure separate, and a dipole moment is formed. For a net polarization to develop, the dipole formed must not be canceled out by other dipoles in the unit cell. Therefore the piezoelectric atomic structure must be non-centrosymmetric. When a piezoelectric material is loaded electrically then the electrical dipoles appear, dipole moment is formed and this results in deformation. The polarization is linear as those shown in Fig. 2.7 and electrical dipoles nucleate only after electrical or mechanical load. The other types of piezoelectric materials are with ferroelectric properties, i.e. spontaneous polarization and electric dipoles exist in their structure even in the absence of electrical field. The piezoelectric effect in ferroelectric is strongly dependent on its atomic structure. Depending on the type of a crystal, a compressive stress can increase or decrease the polarization, or sometimes, have no effect at all. For example, let us consider again the two crystal structures of a traditional piezoelectric ceramic at temperature above and below Curie point, presented in Fig. 2.4. The ceramic phase above Curie point is cubic and has no spontaneous polarization. The ceramic phase below the Curie point is a crystal of tetragonal or rhombohedral symmetry and develops spontaneous

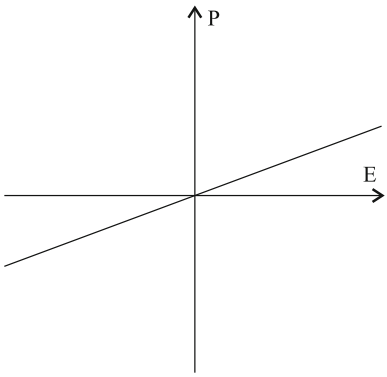

Fig. 2.7 Dielectric polarization

polarization. Piezoelectric properties can be found in the ceramic phase below the Curie point. Materials are polarized along a unique crystallographic direction, in that certain atoms are displaced along this axis, leading to a dipole moment along it. Depending on the crystal system, there may be few or many possible axes. In a crystal, it is likely that dipole moments of the unit cells in one region lie along one of the six directions. Each of these regions is called a domain. A domain is a homogenous region of a ferroelectric, in which all of the dipole moments have the same orientation. In a newly-grown single crystal, there will be many domains, with individual polarizations such that there is no overall polarization. If a mechanical stress is applied to the ferroelectric, then there are domains which will experience an increase in dipole moment and some which will experience a decrease in dipole moment. Overall, there is no net increase in polarization, see Fig. 2.8. This makes BaTiO3 useless as a piezoelectric unless it is put through some additional processing. This process is called *poling*. An electric field is applied to the ferroelectric as it passes through its Curie temperature, so that its spontaneous polarization develops and it is aligned in a single direction. All of the domains in the piezoelectric have a dipole moment pointing in that direction, so there is a net with approximately the same polarization, see Fig. 2.8. When the electric field is removed most of the dipoles are locked in a configuration of near alignment (Fig. 2.8). The full alignment is only possible in a single crystal and in a polycrystalline material there exists still a polarization distribution. The material now has a remanent polarization. The maximum possible value of the remanent polarization is called saturation polarization, i.e. this is the horizontal part of the hysteresis curve in Fig. 2.9. The distinguishing feature of PEM with ferroelectric properties is that the direction of the spontaneous polarization can be reversed by an applied electric field, yielding a hysteresis loop, see Fig. 2.9. The non- linear behavior of the polarization with respect to the applied electrical field consists of three stages which are characterized by:

- reversible domain motion;
- growth of new domains;

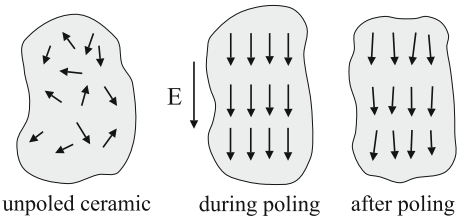

Fig. 2.8 Domain structure of ferroelectric materials and their behavior during poling process

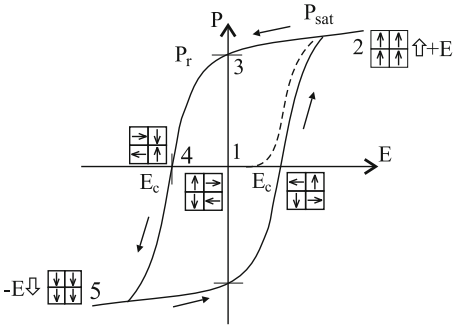

Fig. 2.9 Hysteresis *curve* for polarization of piezoelectric material

- new domains reaching the limit of their growth and reaching the saturation polarization.

Figure 2.9 shows a typical hysteresis curve created by applying an electric field to a piezoelectric ceramic element until the maximum (saturation) polarization P_{sat} is reached, reducing the field to zero determines the remanent polarization P_r reversing the field attains a negative maximum (saturation) polarization and negative remanent polarization, and re-reversing the field restores the positive remanent polarization. When the electric field is the coercive field E_c there is no net polarization due to the mutual compensation of the polarization of different domains.

Summarizing the information of the physical properties of piezoelectric materials presented above, some conclusions can be made:

- PEM is a special type of anisotropic dielectrics where electrical and mechanical fields are coupled due to both the existence of the specific asymmetric atomic structure of the lattice and the existence of spontaneous polarization at the microstructure level;
- The effective usage of both the ferroelectric properties of the piezoelectric ceramics together with the poling process during their manufacture make these materials a basic element in the modern industrial applications.

2.4 Field Equations in 3D

The macroscopic phenomenological theory of piezoelectricity, based on thermodynamic principles, can be traced back to Thompson [36]. However, significant contribution to the theory, as we know it today, was made by Voigt and Duhem. The thermodynamic approach reveals the reversibility and the equivalence of the piezoelectric constants of the direct and converse piezoelectric effects. It is noted that the full thermodynamic derivation should link mechanical, electrical and thermal effects, where the thermo-electric coupling gives rise only to the *pyroelectric* effect. However, since we will not focus on pyroelectricity and as coupling effects are assumed to be linear, the thermal influence can be safely neglected.

2.4.1 Constitutive Equations

For a general piezoelectric material, the total internal energy density U is given by the sum of the mechanical and electrical work done, i.e. in differential form it is

$$dU = \sigma_{ij} ds_{ij} + E_m dD_m. \tag{2.1}$$

Here the mechanical stress σ_{ij} and strain s_{ij} are second rank tensors, E_m is the vector of electric field, D_m is the vector of electrical displacement. All indices run from 1 to 3 and the summation convention over repeated indexes is implied. The polarization vector P_i is introduced to quantify the degree of polarization of the material and it is connected with the vectors of electric field and electrical displacement by the relation, see Parton and Kudryavtsev [29]:

$$D_i = \varepsilon_0 E_i + P_i, \quad P_i = \chi_{ij} E_j. \tag{2.2}$$

In order to derive the constitutive equations of a piezoelectric material different types of thermodynamic potentials can be used as e.g. internal energy $U = U(s_{ij}, D_i)$, the electric Gibbs energy (electric enthalpy) $G_e = G_e(s_{ij}, E_i)$, the Helmholtz free energy $F = F(\sigma_{ij}, D_i)$, the elastic Gibbs energy $G_1(\sigma_{ij}, P_i)$ and the Gibbs free energy $G = G(\sigma_{ij}, E_i)$. The different thermodynamic potentials will facilitate different sets of piezoelectric constitutive formulations, see [10, 15, 20, 29, 37]. Here the constitutive equation derived by using the Gibbs electrical function (electric enthalpy) $G_e(s_{ij}, E_i)$ is presented, assuming it is a quadratic form of s_{ij}, E_i. The Gibbs electrical function is a thermodynamic potential in which the independent variables are the strain deformation s_{ij} and the electrical field E_i, and the dependent flux variables are the stress σ_{ij} and electric displacement (electric flux density) D_i, i.e.

$$dG_e = \left(\frac{\partial G_e}{\partial s_{ij}}\right)_E ds_{ij} + \left(\frac{\partial G_e}{\partial E_m}\right)_s dE_m. \tag{2.3}$$

The differential form of $G_e = U - E_i D_i$, see Ikeda [15], is:

$$dG_e = \sigma_{ij} ds_{ij} - D_m dE_m. \tag{2.4}$$

Comparing Eqs. (2.3) and (2.4) yields

$$\sigma_{ij} = \left(\frac{\partial G_e}{\partial s_{ij}}\right)_E, \quad D_m = -\left(\frac{\partial G_e}{\partial E_m}\right)_s. \tag{2.5}$$

Having in mind that $\sigma_{ij} = \sigma_{ij}(s_{ij}, E_m)$ and $D_i = D_i(s_{ij}, E_m)$, the differentials of stress and electric displacement have the form:

$$d\sigma_{ij} = \left(\frac{\partial \sigma_{ij}}{\partial s_{kl}}\right)_E ds_{kl} + \left(\frac{\partial \sigma_{ij}}{\partial E_m}\right)_s dE_m, \tag{2.6}$$

$$dD_m = \left(\frac{\partial D_m}{\partial s_{kl}}\right)_E ds_{kl} + \left(\frac{\partial D_m}{\partial E_k}\right)_s dE_k. \tag{2.7}$$

The physical meaning of the partial derivatives is as follows:

- $\left(\frac{\partial \sigma_{ij}}{\partial s_{kl}}\right)_E = C_{ijkl}$ is the fourth rank tensor of the elastic stiffness constants at $E = \text{const}$ with $C_{ijkl} = C_{ijlk} = C_{jikl} = C_{klij}$;
- $\left(\frac{\partial \sigma_{ij}}{\partial E_m}\right)_s = -\left(\frac{\partial D_m}{\partial s_{ij}}\right)_E = -e_{ijm}$ is the third rank tensor of the piezoelectric constants at $s_{ij} = \text{const}$ with $e_{kij} = e_{kji}$;
- $\left(\frac{\partial D_m}{\partial E_k}\right)_s = \varepsilon_{mk}$ is the second rank tensor of the dielectric permittivity constants at $s_{ij} = \text{const}$ with $\varepsilon_{ik} = \varepsilon_{ki}$.

In the case of general anisotropy C_{ijkl}, e_{ijm}, ε_{mk} admit 21, 18 and 6 independent components, respectively.

After integration of Eqs. (2.6) and (2.7) at constant partial derivatives the following constitutive equations are obtained:

$$\sigma_{ij} = C_{ijkl} s_{kl} - e_{ijm} E_m, \tag{2.8}$$

$$D_m = e_{mij} s_{ij} + \varepsilon_{mk} E_k. \tag{2.9}$$

The constitutive equations for PEM show coupling between electrical and mechanical quantities. The direct piezoelectric effect or the sensorial effect is described by

Eq. (2.9). This equation shows that an electric polarization and electric field is generated by mechanical stress. The converse effect, or the actuator effect is described by Eq. (2.8) which shows that a PEM undergoes a deformation under an electric field.

The strain-displacement and the electric field-potential relations are given by

$$s_{ij} = \frac{1}{2}(u_{i,j} + u_{j,i}), \quad E_i = -\Phi_{,i}, \tag{2.10}$$

where u_i is the mechanical displacement and Φ is the electrical potential.

The symmetry of the stress tensor enables nine stress components to be reduced to six independent stress components. This also enables the tensor notation to be transformed into a pseudo-tensor form. Using this so-called contracted Voigt subscript notation: $(11) \to 1$, $(22) \to 2$, $(33) \to 3$, $(23) = (32) \to 4$, $(13) = (31) \to 5$, $(12) = (21) \to 6$, the fourth order tensor C_{ijkl} reduces to the matrix representation $C_{\alpha\beta}$ with $(ij) \to \alpha$, $(kl) \to \beta$. In the same way the third order tensor e_{kij} reduces to the matrix representation $e_{k\alpha}$ with $(ij) \to \alpha$. For the analysis of piezoelectric problems it is advantageous to use the notation introduced by Barnett and Lothe [3] and later by [6, 40]. With this notation, the elastic displacement and electric potential, the elastic strain and electric field, the stress and electric displacement, and the elastic and electric coefficients can be grouped as:

- Generalized displacements

$$u_I = \begin{cases} u_i, & I = 1, 2, 3, \\ \Phi, & I = 4 \end{cases} \tag{2.11}$$

- Generalized strain, for $j = 1, 2, 3$,

$$s_{Ij} = \begin{cases} s_{ij}, & I = 1, 2, 3, \\ -E_j, & I = 4. \end{cases} \tag{2.12}$$

- Generalized stresses, for $i = 1, 2, 3$,

$$\sigma_{iJ} = \begin{cases} \sigma_{ij}, & J = 1, 2, 3, \\ D_i, & J = 4. \end{cases} \tag{2.13}$$

- Generalized stiffness matrix for $i, j, k, l = 1, 2, 3$,

$$C_{iJKl} = \begin{cases} C_{ijkl}, & J, K = 1, 2, 3, \\ e_{lij}, & J = 1, 2, 3; , K = 4, \\ e_{ikl}, & J = 4; K = 1, 2, 3, \\ -\varepsilon_{il}, & J = K = 4. \end{cases} \tag{2.14}$$

The symmetry properties of elastic, piezoelectric and dielectric tensors $C_{ijkl}, e_{kij}, \varepsilon_{ij}$ imply the following symmetry property for the extended stiffness tensor:

$$C_{iJKl} = C_{lKJi}. \tag{2.15}$$

In this definition, the lowercase and uppercase subscripts take the values of 1, 2, 3 and 1, 2, 3, 4, respectively. In terms of this shorthand notation, the constitutive relations Eqs. (2.8), (2.9) can be unified into the one single equation

$$\sigma_{iJ} = C_{iJKl} s_{Kl}, \tag{2.16}$$

or in matrix notation

$$\begin{pmatrix} \sigma_{11} \\ \sigma_{22} \\ \sigma_{33} \\ \sigma_{23} \\ \sigma_{31} \\ \sigma_{12} \\ \sigma_{14} \\ \sigma_{24} \\ \sigma_{34} \end{pmatrix} = C \begin{pmatrix} s_{11} \\ s_{22} \\ s_{33} \\ 2s_{23} \\ 2s_{31} \\ 2s_{12} \\ -E_1 \\ -E_2 \\ -E_3 \end{pmatrix}, \tag{2.17}$$

where

$$C = \begin{pmatrix} c_{11} & c_{12} & c_{13} & c_{14} & c_{15} & c_{16} & e_{11} & e_{21} & e_{31} \\ c_{12} & c_{22} & c_{23} & c_{24} & c_{25} & c_{26} & e_{12} & e_{22} & e_{32} \\ c_{13} & c_{23} & c_{33} & c_{34} & c_{35} & c_{36} & e_{13} & e_{23} & e_{33} \\ c_{14} & c_{24} & c_{34} & c_{44} & c_{45} & c_{46} & e_{14} & e_{24} & e_{34} \\ c_{15} & c_{25} & c_{35} & c_{45} & c_{55} & c_{56} & e_{15} & e_{25} & e_{35} \\ c_{16} & c_{26} & c_{36} & c_{46} & c_{56} & c_{66} & e_{16} & e_{26} & e_{36} \\ e_{11} & e_{12} & e_{13} & e_{14} & e_{15} & e_{16} & -\varepsilon_{11} & -\varepsilon_{12} & -\varepsilon_{13} \\ e_{21} & e_{22} & e_{23} & e_{24} & e_{25} & e_{26} & -\varepsilon_{12} & -\varepsilon_{22} & -\varepsilon_{23} \\ e_{31} & e_{32} & e_{33} & e_{34} & e_{35} & e_{36} & -\varepsilon_{31} & -\varepsilon_{32} & -\varepsilon_{33} \end{pmatrix}. \tag{2.18}$$

As discussed in Sect. 2.3, piezoelectric materials show in most cases a crystal structure with a symmetry of hexagonal 6 mm class. In the case that the poling axis coincides with one of the material symmetry axes these materials become transversely isotropic. Transversely isotropic elastic materials are those with an axis of symmetry such that all directions perpendicular to this axis are equivalent. In other words, any plane perpendicular to the axis is a plane of isotropy. In the case of a transversely isotropic solid, the number of the independent elastic, piezoelectric and dielectric constants is 5, 3 and 2 respectively. In this case matrix C in Eq. (2.18) takes the form

$$C = \begin{pmatrix} c_{11} & c_{12} & c_{13} & 0 & 0 & 0 & 0 & 0 & e_{31} \\ c_{12} & c_{11} & c_{13} & 0 & 0 & 0 & 0 & 0 & e_{31} \\ c_{13} & c_{13} & c_{33} & 0 & 0 & 0 & 0 & 0 & e_{33} \\ 0 & 0 & 0 & c_{44} & 0 & 0 & 0 & e_{15} & 0 \\ 0 & 0 & 0 & 0 & c_{44} & 0 & e_{15} & 0 & 0 \\ 0 & 0 & 0 & 0 & 0 & c_{66} & 0 & 0 & 0 \\ 0 & 0 & 0 & 0 & e_{15} & 0 & -\varepsilon_{11} & 0 & 0 \\ 0 & 0 & 0 & e_{15} & 0 & 0 & 0 & -\varepsilon_{11} & 0 \\ e_{31} & e_{31} & e_{33} & 0 & 0 & 0 & 0 & 0 & -\varepsilon_{33} \end{pmatrix}, \tag{2.19}$$

where $c_{66} = \dfrac{1}{2}(c_{11} - c_{12})$

The elasticity coefficients C_{ijkl} and the dielectric constants ε_{ij} are said to be positive-definite if

$$c_{ijkl} q_{ij} q_{kl} > 0, \quad \varepsilon_{il} a_i a_l > 0 \tag{2.20}$$

for any non-zero tensor q_{ij} and any non-zero vector a_i and the following reciprocal symmetries hold due to Eq. (2.16)

$$c_{ijkl} = c_{jikl} = c_{klij}, \quad e_{ijk} = e_{ikj} \quad \varepsilon_{jk} = \varepsilon_{kj}. \tag{2.21}$$

Essentially, these constraints are thermodynamic constraints expressing that the internal energy density must remain positive since this energy must be minimal in a state of equilibrium, see Dieulesaint and Royer [7]. Specializing for the case of transversely isotropic solids, one obtains, see Alshits and Chadwick [2]:

$$c_{11} > |c_{12}|, \quad (c_{11} + c_{12}) c_{33} > 2c_{13}^2, \quad c_{44} > 0, \quad \varepsilon_{11} > 0, \quad \varepsilon_{33} > 0. \tag{2.22}$$

2.4.2 Equations of Motion

The governing equations are given by the equations of motion for the mechanical displacement and by the equations of electrostatic. The electric field that develops in piezoelectrics can assumed to be quasi-static because the velocity of the elastic waves is much smaller than the velocity of electromagnetic waves. Therefore, the magnetic field due to the elastic waves is negligible. This fact implies that the time derivative of the magnetic field B is close to zero, i.e. $\dfrac{\partial B}{\partial t} \approx 0$. Thus one of Maxwell's equations of electrodynamics becomes $\mathrm{rot} E = \dfrac{\partial B}{\partial t} \approx 0$, hence $E = -\mathrm{grad}\Phi$. Consequently, a piezoelectric continuum is based on the governing equations of elastodynamics in the case of small deformations and quasi-electrostatic fields. Restricting to the case

of time-harmonic motion with frequency ω and suppressing the common factor $e^{i\omega t}$ in all terms, the equation of motion read

$$\sigma_{ij,j} + \rho\omega^2 u_i = -b_i, \quad D_{i,i} = -q. \tag{2.23}$$

Here b_i is the body force, ρ is the mass density and q is free electric volume charge. In generalized notation Eq. (2.23) is written as

$$\sigma_{iJ,i} + \rho_{JK}\omega^2 u_K = -F_J, \tag{2.24}$$

where $F_J = (b_i, q)$ and $\rho_{JK} = \begin{cases} \rho, & J, K = 1, 2, 3 \\ 0, & J \text{ or } K = 4 \end{cases}$

The field equations are represented by Eqs. (2.10), (2.16) and (2.24). These group of equations in generalized notation lead to the following equation of motion in the absence of body forces ($b_i = 0$) and free volume charges ($q = 0$)

$$C_{iJKl}u_{K,li} + \rho_{JK}\omega^2 u_K = 0, \quad i, l = 1, 2, 3; \quad J, K = 1, \ldots, 4. \tag{2.25}$$

or in coordinate notation:

$$\begin{cases} c_{11}u_{1,11} + c_{44}u_{1,33} + (c_{13} + c_{44})u_{3,13} + c_{66}u_{1,22} + \dfrac{1}{2}(c_{11} + c_{12})u_{2,12} \\ +(e_{31} + e_{15})u_{4,13} + \rho\omega^2 u_1 = 0, \\ \dfrac{1}{2}(c_{11} + c_{12})u_{1,12} + c_{66}u_{2,11} + c_{11}u_{2,22} + c_{44}u_{2,33} + (c_{13} + c_{44})u_{3,23} \\ +(e_{31} + e_{15})u_{4,33} + \rho\omega^2 u_2 = 0, \\ (c_{13} + c_{44})u_{1,13} + c_{44}(u_{3,11} + u_{3,22}) + c_{33}u_{3,33} + (c_{13} + c_{44})u_{2,23} \\ +e_{15}(u_{4,11} + u_{4,22}) + e_{33}u_{4,33} + \rho\omega^2 u_3 = 0, \\ (e_{15} + e_{31})u_{1,13} + e_{15}(u_{3,11} + u_{3,22}) + e_{33}u_{3,33} + (e_{31} + e_{15})u_{3,23} \\ -\varepsilon_{11}u_{4,11} - \varepsilon_{11}u_{4,22} - \varepsilon_{33}u_{4,33} = 0. \end{cases} \tag{2.26}$$

Note that there is no time rate in the last equation due to the quasi-electrostatic approximation, i.e. the absence of magnetization. This means that frequency dependence is induced only by the mechanical displacement u_i.

The reason to show simultaneously the equations in generalized notation (2.25) and in coordinate notation (2.26) is that for the derivation of the fundamental solutions in Chap. 3, it is better to use a coordinate notation, while for the derivation of the integro–differential equations and for explaining the numerical solution by BIEM in Chap. 4, it is better to use the generalized notation.

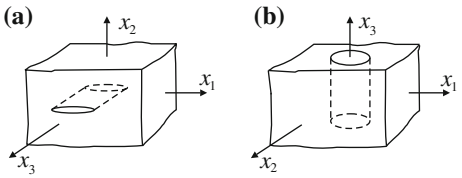

Fig. 2.10 Location of the defect in a Cartesian coordinate system $Ox_1x_2x_3$: **a** anti-plane deformation state, **b** in-plane deformation state

2.5 Field Equations in 2D

The equations of motion simplify considerably when "in-plane" or "anti-plane" problems are considered. For this purpose a Cartesian coordinate system $Ox_1x_2x_3$, see Fig. 2.10 is used. Assume that PEM shows hexagonal symmetry with respect to the Ox_3 axis and the poling axis is collinear with the Ox_3 axis. The plane Ox_1x_2 then is the isotropic plane. In what follows we will consider two coupled plane problems that are obtained from the 3D stress–strain state described in Sect. 2.4. The uncoupling of equations that would allow us to study the in-plane and anti-plane problems separately is only possible if the material is monoclinic. Fortunately the piezoelectric materials belong to this group of materials.

2.5.1 In-plane Piezoelectric Equations

Assumed is an electromechanical load as follows:

- the electric field is applied in the plane Ox_1x_3, i.e. $E_1 \neq 0$, $E_3 \neq 0$, $E_2 = 0$ and also corresponding electrical displacements are $D_1 \neq 0$, $D_3 \neq 0$, $D_2 = 0$, see Fig. 2.10a;
- the mechanical load is also in the plane Ox_1x_3 and the mechanical displacements are $u_1 \neq 0, u_3 \neq 0$, $u_2 = 0$. The nonzero stress and strain components are $\sigma_{11}, \sigma_{33}, \sigma_{13}$ and s_{11}, s_{33}, s_{13}.

2.5.1.1 Constitutive Equations

The constitutive equations are obtained from Eqs. (2.16):

$$\sigma_{iJ} = C_{iJKl}s_{Kl}, \quad i, j, l = 1, 3; J, K = 1, 3, 4. \tag{2.27}$$

or in matrix notation

$$\begin{pmatrix} \sigma_{11} \\ \sigma_{33} \\ \sigma_{31} \\ \sigma_{14} \\ \sigma_{34} \end{pmatrix} = C \begin{pmatrix} s_{11} \\ s_{33} \\ 2s_{31} \\ -E_1 \\ -E_3 \end{pmatrix}, \tag{2.28}$$

where

$$C = \begin{pmatrix} c_{11} & c_{13} & 0 & 0 & e_{31} \\ c_{13} & c_{33} & 0 & 0 & e_{33} \\ 0 & 0 & c_{44} & e_{15} & 0 \\ 0 & 0 & e_{15} & -\varepsilon_{11} & 0 \\ e_{31} & e_{33} & 0 & 0 & -\varepsilon_{33} \end{pmatrix}, \tag{2.29}$$

and in coordinate notation

$$\begin{aligned} \sigma_{11} &= c_{11}u_{1,1} + c_{13}u_{3,3} - e_{31}E_3, \\ \sigma_{33} &= c_{13}u_{1,1} + c_{33}u_{3,3} - e_{33}E_3, \\ \sigma_{13} &= c_{44}u_{1,3} + c_{44}u_{3,1} - e_{15}E_1, \\ D_1 &= e_{15}u_{1,3} + e_{15}u_{3,1} + \varepsilon_{11}E_1, \\ D_3 &= e_{31}u_{1,1} + e_{33}u_{3,3} + \varepsilon_{33}E_3. \end{aligned} \tag{2.30}$$

The strain-displacement and the electric field-potential relations are

$$s_{ij} = \frac{1}{2}(u_{i,j} + u_{j,i}), \quad E_i = -\Phi_{,i}, \quad i, j = 1, 3. \tag{2.31}$$

and the generalized displacement is $u_K = (u_1, u_3, \Phi)$.

2.5.1.2 Equation of Motion

The equations of in-plane coupled motion in the Ox_1x_3 plane is obtained from Eq. (2.25)

$$C_{iJKl}u_{K,li} + \rho_{JK}\omega^2 u_K = 0, \quad i, l = 1, 3; \quad J, K = 1, 3, 4. \tag{2.32}$$

and in coordinate notation

$$\begin{cases} c_{11}u_{1,11} + c_{44}u_{1,33} + (c_{13} + c_{44})u_{3,13} + (e_{31} + e_{15})u_{4,13} + \rho\omega^2 u_1 = 0, \\ (c_{13} + c_{44})u_{1,13} + c_{44}u_{3,11} + c_{33}u_{3,33} + e_{15}u_{4,11} + e_{33}u_{4,33} + \rho\omega^2 u_3 = 0, \\ (e_{15} + e_{31})u_{1,13} + e_{15}u_{3,11} + e_{33}u_{3,33} - \varepsilon_{11}u_{4,11} - \varepsilon_{33}u_{4,33} = 0. \end{cases} \tag{2.33}$$

Equations of motion (2.32) and (2.33) govern the solution of the 2D coupled in-plane electro-elastic problem, when the displacement and electric field are both in-plane.

2.5.2 Anti-plane Piezoelectric Equations

The electromechanical load is prescribed as follows:

- mechanical load is out of plane Ox_1x_2 and the mechanical displacements are $u_1 = 0, u_2 = 0, u_3 \neq 0$. The nonzero stress and strain components are σ_{13}, σ_{23} and s_{13}, s_{23}, see Fig. 2.10b.
- electric field is applied in plane Ox_1x_2, i.e. $E_1 \neq 0, E_2 \neq 0, E_3 = 0$ and also the corresponding electrical displacements are $D_1 \neq 0, D_2 \neq 0, D_3 = 0$.

2.5.2.1 Constitutive Equations

The constitutive equations are obtained from Eq. (2.16):

$$\sigma_{iJ} = C_{iJKl} s_{Kl}, \quad i, j, l = 1, 2; J, K = 3, 4. \tag{2.34}$$

or in coordinate notation

$$\begin{aligned} \sigma_{13} &= c_{44} u_{3,1} - e_{15} E_1 \\ \sigma_{23} &= c_{44} u_{3,2} - e_{15} E_2, \\ D_1 &= e_{15} u_{3,1} + \varepsilon_{11} E_1, \\ D_2 &= e_{15} u_{3,2} + \varepsilon_{11} E_2, \end{aligned} \tag{2.35}$$

where

$$\begin{pmatrix} \sigma_{13} \\ \sigma_{23} \\ \sigma_{14} \\ \sigma_{24} \end{pmatrix} = C \begin{pmatrix} s_{13} \\ s_{23} \\ -E_1 \\ -E_2 \end{pmatrix}, \quad C = \begin{pmatrix} c_{44} & e_{15} \\ e_{15} & -\varepsilon_{11} \end{pmatrix}. \tag{2.36}$$

2.5.2.2 Equation of Motion

The equation of anti-plane coupled motion in Ox_1x_2 plane is obtained by Eq. (2.25)

$$C_{iJKl} u_{K,li} + \rho_{JK} \omega^2 u_K = 0, \quad i, l = 1, 2; \quad J, K = 3, 4. \tag{2.37}$$

where the generalized displacement is $u_K = (u_3, \Phi)$. In coordinate notations Eq. (2.37) is

$$\begin{cases} c_{44}\triangle u_3 + e_{15}\triangle u_4 + \rho\omega^2 u_3 = 0, \\ e_{15}\triangle u_3 - \varepsilon_{11}\triangle u_4 = 0 \end{cases}. \tag{2.38}$$

where $\triangle = \partial^2_{x_1} + \partial^2_{x_2}$ is Laplace operator.

Equations of motion (2.37) and (2.38) govern the solution of the 2D coupled in-plane piezoelectric problem, when the displacement field is out of plane and the electric field is in-plane.

2.6 2D Domains with Cracks

2.6.1 Wave Propagation

Wave propagation in a media with defects, if there are no other sources of dissipation, is accompanied by wave phenomena as:

- *diffraction*, revealing the wave deviation from original wave path due to the superposition of incident and scattered wave;
- *scattering* refers to the wave radiation from defects acting as secondary sources of radiation due to the excitation of the incident wave;
- *attenuation*, i.e. the amplitude of the incident wave diminishes because during the diffraction and scattering process, a part of the incident wave energy is converted into the energy of diffracted and scattered waves;
- *dispersion*, that is energy (wave shape) distortion due to the frequency dependence of the effective wave phase velocity.

Interaction mechanism between waves and defects depend on the relation between the size c of the defect and the wavelength λ, i.e. the wave is not sensitive to the defect if $c \ll \lambda/2$. Wave scattering and diffraction is dominant at $c \approx \lambda$ and wave reflection and refraction is being realized at $c \gg \lambda$. The defects as cracks or holes are not only wave refractors and scatterers but they acts also as stress concentrators.

The evaluation of wave field distortion produced by a defect is a process studied in nondestructive testing of materials and structures, wave propagation theory with its application in seismology, modern engineering and medicine. The obstacle can be an inclusion, a hole, a crack or any existing boundary. Also, the fracture mechanics approach can be applied to the continua with existing defects like cracks and holes for assessing the initiation, growth, stability of the crack state and respectively to evaluate the resistance of the studied material or engineering structure.

In the following sections the basic 2D mechanical models describing time-harmonic wave propagation in homogeneous piezoelectric solid with cracks and holes are formulated. We are considering finite internal cracks with a straight or an

arc shape in a simply connected domain (unbounded or bounded) or in a domain with holes.

2.6.2 Fracture Mechanics Approach

Fracture mechanics provides a theoretical background for materials and structures containing cracks and faults. Stress intensity factors are key parameters in crack analysis. The classical work of Irwin [16] showed that the coefficients of the dominant singular term in the near-field solution for the stresses at the crack tip are directly related to the energy release rate (the energy released per unit of crack extension). These coefficients are referred to as the stress intensity factors. Generalized SIFs, play a dominate role because they characterize the intensity of the singular piezoelectric crack field (generalized stress and strain). The knowledge of SIFs is based on the near-field solutions and it is useful because it gives information for the strength and life time prediction of the studied solids and structures.

As can be seen from the field equations discussed in Sects. 2.4 and 2.5 we restrict our attention to the sufficiently small loading range which in a good approximation can be characterized by a linear material model with a constant polarization field. In this case we can apply the concepts of linear fracture mechanics generalized to treat the piezoelectric materials. The aim is to evaluate the influence of the electro-mechanical loads on the fracture behaviour of cracked piezoelectric solids. Following [12, 19, 27, 28, 32, 33, 35] the near-field solutions for typical crack opening mode, (see Fig. 2.11) can be expressed in polar coordinates with the origin at the crack-tip (see Fig. 2.12), as

$$\begin{aligned} \sigma_{iJ}(r,\theta,\omega) &= \frac{1}{\sqrt{r}} K_H(\omega) f_{iJ}^H(\theta), \\ u_J(r,\theta,\omega) &= \sqrt{r} K_H(\omega) g_{iJ}^H(\theta), \end{aligned} \tag{2.39}$$

where $H = I, \ldots, IV$, and the generalized stresses behave singular as $O(1/\sqrt{r})$, whereas the generalized displacements behaves as $O(\sqrt{r})$ for $r \to 0$. The angular functions $f_{iJ}^H(\theta)$, $g_{iJ}^H(\theta)$ depend only on the material constants. The coefficients K_I, K_{II} and K_{III} are the mechanical stress intensity factors, which are complemented by the new forth "electric" intensity factor K_{IV}, that characterizes the electric field singularity. In the general case the stresses and displacements are the sum of the four terms and they can only be separated in specific loading cases. Note that the behaviour of the stresses and displacements near the crack-tip is fully prescribed by the theoretical study of the asymptotic behaviour of solutions of elliptic boundary value problems in the domain with singularities, like angular points, see Kondratiev [19]. Correspondingly the K-factors K_H are coefficients of the representation of the solution near the crack-tip. From Eq. (2.39) the following conclusions can be drawn:

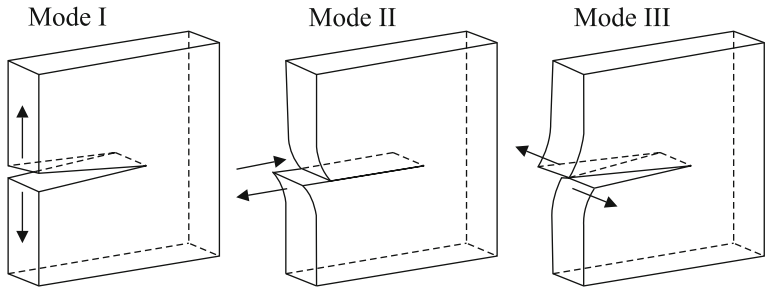

Fig. 2.11 Crack opening modes

Fig. 2.12 Stress components and reference system in the neighborhood of the crack

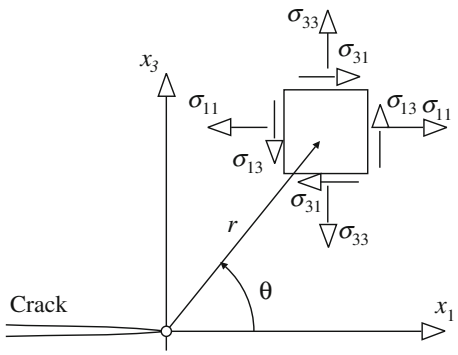

- The mutual interdependence between mechanical and electrical crack tip parameters;
- Angular functions f_{iJ}^H, g_J^H do not depend on the applied load and the domain geometry;
- The generalized SIFs K_H depend strongly on the applied load.

The numerical calculation of the SIFs is based on then well-known displacement or traction formulae, see [1, 12, 35, 43]. The traction formulae will be explained and used here.

Consider an in-plane crack along the segment AB with local coordinate of points $A(-c, 0)$, $B(c, 0)$ in the plane Ox_1x_3 and subjected to an electro-mechanical load in the crack plane. The following expressions for the generalized K-factors are obtained in this case, see [1, 41]:

$$\begin{aligned} K_I &= \lim_{x_1 \to \pm c} t_3 \sqrt{2\pi(x_1 \mp c)}, \\ K_{II} &= \lim_{x_1 \to \pm c} t_1 \sqrt{2\pi(x_1 \mp c)}, \\ K_{IV} &= \lim_{x_1 \to \pm c} t_4 \sqrt{2\pi(x_1 \mp c)}, \end{aligned} \tag{2.40}$$

where t_J is the traction at a point close to the crack-tips.

For an anti-plane crack subjected to mechanical load out of plane $x_3 = 0$ and electrical load in the plane $x_3 = 0$ the corresponding formulae are:

$$\begin{aligned} K_{III} &= \lim_{x_1 \to \pm c} t_3 \sqrt{2\pi (x_1 \mp c)}, \\ K_{IV} &= \lim_{x_1 \to \pm c} t_4 \sqrt{2\pi (x_1 \mp c)}. \end{aligned} \tag{2.41}$$

2.6.3 Boundary Value Problems

Selection of the adequate boundary condition on the crack faces in piezoelectric fracture mechanics has been discussed over the past 2 decades. It is a well-known fact that there are discrepancies between the experimental measurements and the theoretical predictions based on linear piezoelectric crack models. The character of the electrical boundary conditions is discussed in a number of papers, see [8, 9, 11, 14, 21, 23–25, 30, 32, 34, 42], etc.

Different types of crack surface boundary conditions belonging to the linear models are addressed:

- impermeable crack with mechanical traction-free surface;
- permeable crack with mechanical traction-free surface;
- limited permeable crack or deformation dependent electrical PKHS (PartonKudryavtsevHaoShen) boundary condition with mechanical traction-free surface;
- energetically consistent cracks with mechanical non-traction-free surface.

The BIEM that we apply for the numerical study of crack problems in 2D piezoelectric domains is a linear method—i.e. it presumes a linear boundary value problem. Therefore, we will deal in most cases with impermeable or permeable electrical boundary conditions along the crack line. Under some additional restrictions, the limited permeable cracks can also be considered. The detailed description of the electric boundary conditions together with comparative numerical studies is provided in Chap. 9. In the following we formulate the basic boundary-value problems for the in-plane and anti-plane problems of Sect. 2.5 that will be solved numerically with BIEM.

With respect to the domain we consider two types of BVP for cracks—(i) in bounded domains, and (ii) in infinite domains. The problem (i) aims to estimate the global behaviour of the solution in the presence of cracks in the domain and to evaluate the dependance of the SIFs on the geometry parameters of the external boundary. Such a problem is related to the eigenvalue problem and correspondingly to inverse problems. The solution of the problem (ii) gives an information about the local behaviour of the wave field near the cracks and the evaluation of the SIFs.

Denote by G a bounded domain with smooth boundary $S = \partial G$ in the plane $R^2 = Ox_1x_3$ for the in-plane case and $R^2 = Ox_1x_2$ for the anti-plane case and by $S_{cr} = S_{cr}^+ \cup S_{cr}^-$ an internal crack—an open arc. Suppose that $S = S_u \cup S_t$, $S_u \cap S_t = \emptyset$ and that there are prescribed displacements, $\bar{u}_J$ on S_u and prescribed tractions $\bar{t}_J$ on S_t.

The BVP in G with impermeable boundary conditions on S_{cr} is defined as

$$\begin{vmatrix} \sigma_{iJ,i} + \rho_{JK}\omega^2 u_K = 0 \quad \text{in } G\backslash S_{cr}, \\ u_J|_{S_u} = \bar{u}_J, \quad t_J|_{S_t} = \bar{t}_J, \\ t_J|_{S_{cr}} = 0. \end{vmatrix} \tag{2.42}$$

Solution of Eq. (2.42) is a vector-valued function with components $u_J \in C^2(G\backslash S_{cr})$ that satisfies the equation and boundary conditions. We will transform the problem (2.42) in Chap. 4 into an integro–differential equation on $S \cup S_{cr}$ with the unknowns u_J on S_t; t_J on S_u and the jump of displacement across the crack line, i.e. the crack opening displacement $\Delta u_J = u_J|_{S_{cr}^+} - u_J|_{S_{cr}^-}$.

The BVP in G with permeable boundary conditions on S_{cr} is defined as

$$\begin{vmatrix} \sigma_{iJ,i} + \rho_{JK}\omega^2 u_K = 0 \quad \text{in } G\backslash S_{cr}, \\ u_J|_{S_u} = \bar{u}_J, \quad t_J|_{S_t} = \bar{t}_J, \\ t_i|_{S_{cr}} = 0, \quad u_4|_{S_{cr}^+} = u_4|_{S_{cr}^-}. \end{vmatrix} \tag{2.43}$$

Solution of Eq. (2.43) is a vector-valued function with components $u_J \in C^2(G\backslash S_{cr})$ that satisfies the equation and boundary conditions. In Chap. 4 after the transformation of the problem (2.43) into an integro–differential equation on $S \cup S_{cr}$, the unknowns are: u_J on S_t; t_J on S_u, the crack opening displacement Δu_i and t_4 on S_{cr}.

The BVP in the plane $R^2 = Ox_1x_3$ for the in-plane case and $R^2 = Ox_1x_2$ for the anti-plane case with impermeable boundary conditions on S_{cr} is defined as

$$\begin{vmatrix} \sigma_{iJ,i} + \rho_{JK}\omega^2 u_K = 0 \quad \text{in } R^2\backslash S_{cr}, \\ t_J|_{S_{cr}} = 0. \end{vmatrix} \tag{2.44}$$

In addition the unknown u_J must satisfies the Sommerfeld's type condition at infinity, see Sommerfeld [31]. Solution of Eq. (2.44) is a vector-valued function with components $u_J \in C^2(R^2\backslash S_{cr})$ that satisfies the equation and boundary condition. In Chap. 4 after the transformation of the problem (2.44) into an integro–differential equation on S_{cr}, the unknown is the crack opening displacement $\Delta u_J = u_J|_{S_{cr}^+} - u_J|_{S_{cr}^-}$.

The BVP in the plane $R^2 = Ox_1x_3$ for the in-plane case and $R^2 = Ox_1x_2$ for the anti-plane case with permeable boundary conditions on S_{cr} is defined as

$$\begin{vmatrix} \sigma_{iJ,i} + \rho_{JK}\omega^2 u_K = 0 \quad \text{in } R^2\backslash S_{cr}, \\ t_i|_{S_{cr}} = 0, \quad u_4|_{S_{cr}^+} = u_4|_{S_{cr}^-} \end{vmatrix} \tag{2.45}$$

In addition the unknown u_J must satisfies the Somerfield type condition at infinity. Solution of Eq. (2.45) is a vector-valued function with components $u_J \in C^2(R^2\backslash S_{cr})$ that satisfies the equation and boundary condition. In Chap. 4 after the transformation of the problem (2.45) into an integro–differential equation on S_{cr}, the unknown is the crack opening displacement Δu_i and t_4.

Note that the field equations for the in-plane case, are prescribed in Sect. 2.5.1 for $i = 1, 3, J, K = 1, 3, 4$, while field equations for the anti-plane case are in Sect. 2.5.2 for $i = 1, 2, J, K = 3, 4$.

The non-hypersingular traction BIEM and its numerical solution are discussed in Chap. 4. Different illustrative numerical examples are presented in Chaps. 5–15, where we consider uncoupled problems, multiple cracks and dynamic crack interaction phenomena, unbounded and bounded domains, inhomogeneous domains, domains with hole or crack and hole. For every particular case the BVP will be stated together with the corresponding boundary integral equation formulation.

References

1. Aliabadi AM, Rooke D (1991) Numerical fracture mechanics. Computational Mechanics, Southampton
2. Alshits VIA, Chadwick P (1997) Concavities on the zonal slowness section of a transversely isotropic elastic material. Wave Motion 25:347–359
3. Barnett DM, Lothe J (1975) Dislocations and line charges in anisotropic piezoelectric insulators. Physica Status Solidi B76:105–111
4. Curie J, Curie P (1880a) Développement, par pression, de l'électricité polaire dans les cristaux hémièdres faces ' inclinées. C R Acad Sci Gen 91:294–295
5. Curie J, Curie P (1880b) Sur l'électricité polaire dans les cristaux hémièdres ' faces inclinées. C R Acad Sci Gen 91:383–386
6. Davi G, Milazzo A (2001) Multidomain boundary integral formulation for piezoelectric materials fracture mechanics. Int J Solids Struct 38:7065–7078
7. Dieulesaint E, Royer D (1974) Elastic wave in solids. Wiley, New York
8. Dunn ML (1994) Electroelastic Green's functions for transversely isotropic piezoelectric media and their application to the solution of inclusion and ingomogeneity problems. Int J Eng Sci 32(1):119–131
9. Enderlein M, Ricoeur A, Kuna M (2005) Finite element technique for dynamic crack analysis in piezoelectrics. Int J Fract 134:191–208
10. Eringen AC, Maugin GA (1990) Electrodynamics of continua I: foundations and solid media. Springer, Berlin
11. Gao C, Fan W (1999) A general solution for the plane problem in piezoelectric media with collinear cracks. Int J Eng Sci 37:347–363
12. Gross D, Seelig T (2011) Fracture mechanics: with an introduction to micromechanics. Springer, Berlin
13. Hankel WG (1881) Uber die aktinound piezoelektrischen eigen schaften des bergkrystalles und ihre beziehung zi den thermoelektrischen. Abh Sachs 12:457
14. Hao TH, Shen ZY (1994) A new electric boundary condition of electric fracture mechanics and its applications. Eng Fract Mech 47:793–802
15. Ikeda T (1990) Fundamentals of piezoelectricity. Oxford University Press, Oxford
16. Irwin GR (1957) Analysis of stresses and strains near the end of a crack traversing a plate. J Appl Mech 24:361–364
17. Jaffe B, Roth RS, Marzullo S (1954) Piezoelectric properties of lead zirconate-lead titanate solid-solution ceramic ware. J Appl Phys 25:809–810
18. Kawai H (1969) Japanese. J Appl Phys 8:975
19. Kondratiev V (1967) Boundary problems for elliptic equations in domain with conocal and angular points. In: Proceedins of the Moscow mathematical society, vol 16. pp 227–313
20. Landau DL, Lifshitz EM (1960) Electrodynamics of continuous media. Pergamon Press, Oxford

21. Landis CM (2004) Energetically consistent boundary conditions for electromechanical fracture. Int J Solids Struct 41:6241–6315
22. Lippman G (1881) Principe de la conservation de l'électricité. Ann Chimie Phys 24:145
23. McMeeking RM (1989) Electrostrictive stresses near crack-like flaws. J Appl Math Phys 40:615–627
24. McMeeking RM (1999) Crack tip energy relase rate for a piezoelectric compact tension specimen. Eng Fract Mech 64:217–244
25. McMeeking RM (2004) The energy release rate for a Griffith crack in a piezoelectric material. Eng Fract Mech 71:1149–1163
26. Newnham RE (1980) Composite piezoelectric transducers. Mater Eng 2:93–106
27. Pak YE (1992b) Linear electro-elastic fracture mechanics of piezoelectric materials. Int J Fract 54:79–100
28. Park SB, Sun CT (1995) Effect of electric field on fracture of piezoelectric ceramics. Int J Fract 70(3):203–216
29. Parton VZ, Kudryavtsev BA (1988) Electromagnetoelasticity. Gordon and Breach Science, New York
30. Shindo Y, Murakami H, Horiguchi K, Narita F (2002) Evaluation of electric fracture properties of piezoelectric ceramics using the finite element and single-edge precracked beam methods. J Am Ceramic Soc 85:1243–1248
31. Sommerfeld A (1949) Partial differential equations in physics. Academic Press, New York
32. Sosa H (1991) Plane problems in piezoelectric media with defects. Int J Solids Struct 28:491–505
33. Sosa H (1992) On the fracture mechanics of piezoelectric solids. Int J Solids Struct 29:2613–2622
34. Sosa H, Khutoryansky N (1996) New developments concerning piezoelectric materials with defects. Int J Solids Struct 33:3399–3414
35. Suo Z, Kuo C, Barnett D, Willis J (1992) Fracture mechanics for piezoelectric ceramics. J Mech Phys Solids 40:739–765
36. Thompson W (1878) On the thermoelastic, thermomagnetic and puro-electric properties of matter. Phil Mag 5:4–27
37. Tiersten HF (1969) Linear piezoelectric plate vibrations. Plenum Press, New York
38. Valasek J (1920) Piezoelectric and allied phenomena in Rochelle salt. Phys Rev 15:537
39. Voigt W (1910) Lehrbuch der Kristallphysik. Teubner, Leipzig
40. Wang CY, Zhang Ch (2005) 2 D and 3 D dynamic Green's functions and time-domain BIE formulations for piezoelectric solids. Eng Anal Bound Elem 29:454–465
41. Wang X, Yu S (2001) Transient response of a crack in a piezoelectric strip subjected to the mechanical and electrical impacts: mode- I problem. Mech Mater 33:11–20
42. Xu LY, Rajapakse RKND (2001) On a plane crack in piezoelectric solids. Int J Solids Struct 38:7643–7658
43. Zhang C, Gross D (1998) On wave propagation in elastic solids with cracks. Computational Mechanics, Southampton

Springer

http://www.springer.com/978-3-319-03960-2

Dynamic Fracture of Piezoelectric Materials
Solution of Time-Harmonic Problems via BIEM
Dineva, P.S.; Gross, D.; Müller, R.; Rangelov, T.

2014, XIV, 249 p. 119 illus., Hardcover
ISBN: 978-3-319-03960-2